The evolution of radio sources in the UKIDSS-DXS XMM-LSS field

Kim McAlpine[1] and Matt J. Jarvis[2,3]

[1] *Department of Physics and Electronics, Rhodes University, Grahamstown, 6139, South Africa*
[2] *Centre for Astrophysics, Science & Technology Research Institute, University of Hertfordshire, Hatfield, Herts, AL10 9AB, UK*
[3] *Physics Department, University of the Western Cape, Cape Town, 7535, South Africa*

15 December 2010

ABSTRACT

We investigate the cosmic evolution of low luminosity ($L_{1.4\,\mathrm{GHz}} < 10^{25}\,\mathrm{W\ Hz^{-1}sr^{-1}}$) radio sources in the XMM Large Scale Structure survey field (XMM-LSS). We match low frequency selected (610 MHz) radio sources in the XMM-LSS field with near infrared K-band observations over the same field from the UKIRT Infrared Deep Sky Survey. We use both the mean V/V_{max} statistic and the radio luminosity function of these matched sources to quantify the evolution of the co-moving space density of the low luminosity radio sources in our sample. Our results indicate that the low luminosity sources evolve differently to their high luminosity counterparts out to a redshift of z∼0.8. The derived luminosity function is consistent with an increase in the co-moving space density of low luminosity sources by a factor of ∼1.5 at z=0.8. We show that the use of the $K - z$ diagram for the radio source population, although coarser than a full photometric redshift analysis, produces consistent results with previous studies using ∼> 10 band photometry. This offers a promising method for conducting similar analyses over the whole sky with future near- and mid-infrared surveys.

Key words: galaxies: active, galaxies: luminosity function, radio continuum: galaxies

1 INTRODUCTION

The strong cosmic evolution of the most powerful radio sources was first deduced by Longair (1966) from low frequency radio source counts. This evolution has since been confirmed by a number of investigations which imply that the co-moving space density of high luminosity radio sources has decreased by a factor of approximately 1000 between $z \sim 2$ and $z \sim 0$ (e.g. Laing, Riley & Longair 1983; Dunlop & Peacock 1990; Willott et al. 2001). Beyond $z \sim 2$ the evolution remains uncertain (e.g. Jarvis & Rawlings 2000; Jarvis et al. 2001b) but appears to undergo a gradual decline (e.g. Wall et al. 2005). The evolution of the low-power radio sources is less well constrained, but early studies of the radio source counts indicated that the low luminosity sources could not be evolving as strongly as their high luminosity counterparts (Longair 1966; Doroshkevich, Longair & Zeldovich 1970). Many models of the evolution of radio sources thus divide the radio source population into two independently evolving components, a strongly evolving high luminosity component and a lower luminosity component with much weaker evolution (e.g. Jackson & Wall 1999; Willott et al. 2001).

Radio galaxies can be classified into two morphologically distinct groups identified as Fanaroff-Riley class I (FRI) and Fanaroff-Riley class II (FRII) sources (Fanaroff & Riley 1974). The FRI sources have higher surface brightness close to the centre of their radio lobes whereas the FRII sources have highly collimated large-scale jets and bright emission hotspots at the edges of their radio lobes. The FRII sources are typically more luminous than the FRI sources with the division in luminosity falling at roughly $L_{1.4\,\mathrm{GHz}} = 10^{25}$ W Hz^{-1}sr^{-1}. This dividing luminosity may be dependent on the optical luminosity of the host galaxy, a higher optical host luminosity results in a higher FRI/FRII division luminosity (Ledlow & Owen 1996). It has been suggested that the FRI and FRII sources might respectively be associated with the slowly and rapidly evolving components of the radio source population (Jackson & Wall 1999). However Rigby et al. (2007) find evidence that high luminosity FRI sources evolve as rapidly as FRII sources of comparable radio power. Furthermore, Gendre, Best & Wall (2010) performed a detailed comparison of the radio luminosity function of FRI and FRII sources at a number of redshifts. This analysis revealed that both populations expe-

rience luminosity dependent number density enhancements at higher redshifts, z≈0.8∼2.5, and that there were no significant differences between the enhancements measured for these two populations. These results would seem to suggest that both types of FR sources experience a common evolutionary history and thus cannot fully account for the observed dichotomy in cosmic evolution.

Recent evidence suggests that a more important division in the radio source population, distinct from the morphological classification, may be related to different modes of black hole accretion. Radio galaxies have also been classified according to the presence or absence of narrow high-excitation emission lines in the spectra of their optical host galaxies (Hine & Longair 1979; Laing et al. 1994; Jackson & Rawlings 1997; Willott et al. 2001). Objects without high-excitation emission lines are referred to as low-excitation radio galaxies (LERG). Low luminosity FRI galaxies are predominantly LERG's and most objects with high excitation emission lines are associated with the more powerful FRII sources. However the relationship between FR class and the emission line classification scheme is not one-to-one as many FRII galaxies have been found to be low-excitation radio galaxies (e.g. Evans et al. 2006). It has been argued that these two groups correspond to different AGN phenomena powered by fundamentally different modes of accretion. The LERG sources are powered by a radiatively inefficient accretion of the hot gas in the intergalactic medium, referred to as "radio" mode accretion. While the HERG are powered by radiatively efficient accretion of cold gas, referred to as quasar mode accretion (Evans et al. 2006; Hardcastle, Evans & Croston 2006, 2007; Herbert et al. 2010). Smolčić et al. (2009) argue that the observed bimodal evolution of radio sources may be caused by differences in the evolution of these black hole accretion modes.

Understanding the relationships between different classes of radio galaxies, and their cosmic evolution, is important for understanding models of galaxy formation and evolution. Semi-analytic models of hierarchical galaxy formation predict that galaxies in the local universe should be more massive and have higher rates of star formation than is observed (Bower et al. 2006). There is increasing observational evidence that radio activity from AGN may disrupt cooling flows in luminous early-type galaxies thus slowing or preventing significant accretion of gas and further star formation (Fabian et al. 2003; Bîrzan et al. 2004; Rawlings & Jarvis 2004). This negative AGN feedback has been successfully incorporated into models of galaxy formation which are then able to better reproduce several features of the observed universe including the exponential cut-off in the bright end of the galaxy luminosity function (Croton et al. 2006; Bower et al. 2006). Best et al. (2006) implied that the low luminosity radio sources may be the predominant contributors to this negative feedback effect.

Current studies of the cosmic evolution of low power radio sources seem to imply that these sources are not evolving at all or experience only mild negative evolution. Clewley & Jarvis (2004) found that the low luminosity radio sources with $L_{325MHz} < 10^{25}$ W Hz^{-1}sr^{-1} exhibit no evolution out to redshift $z \sim 0.8$, Waddington et al. (2001) also found no evidence of evolution in their study of 72 sources. Sadler et al. (2007) find evidence of mild evolution out to

$z \sim 0.7$ in their comparison of the radio luminosity function of sources in the 2dF-SDSS Luminous Red Galaxy (2SLAQ) and QSO survey with that of sources in the 6dF Galaxy survey (6dFGS). This was consistent with pure luminosity evolution of the form $(1 + z)^{2.0 \pm 0.3}$ which ruled out the no evolution scenario at the 6σ level. Donoso, Best & Kauffmann (2009) also find evidence of mild positive evolution in the $z = 0.1 \sim 0.55$ redshift range. Using radio sources in the VLA-COSMOS survey Smolčić et al. (2009) find evidence that this mild evolution continues out to $z \sim 1.3$. All of these studies imply that the level of evolution in the low power radio sources is significantly less than that taking place in the high luminosity sources.

In this study we use low frequency radio sources detected in the XMM-Large Scale Structure survey field to investigate the co-moving space density of low-luminosity radio sources. The low-frequency selection is preferred over high-frequency (e.g. ≥ 1.4 GHz), as it provides an orientation independent selection, as the low-frequency detects the optically-thin lobe emission, whereas high-frequency surveys contain a higher fraction of pole-on sources where the optically thick core dominates (e.g. Jarvis & McLure 2002).

In section 2 and 3 we discuss the radio and optical observations used in our analysis. Section 4 outlines the method we used to cross match the radio sources with their optical counterparts. In section 5 we describe the method used to obtain redshifts for our sample. In the section 6 and 7 we discuss the V/V_{max} statistic used to quantify the evolution of our sources. In section 8 we determine the radio luminosity function of the low luminosity sources in our observed field and use it to investigate their evolution. We present our conclusions in section 9.

We assume the $H_0=70$ km.s^{-1}.Mpc^{-1} and a $\Omega_M=0.3$ and $\Omega_\Lambda=0.7$ cosmology throughout this paper.

2   RADIO DATA AT 610 MHZ

We use the radio observations of the XMM-LSS field described in detail in Tasse et al. (2007). These observations cover 13 degrees^2 centered at α(J2000)=$2^h24^m00^s$ and δ(J2000)=-4°09'47''. This field was observed for a total of 18 h with Giant Metrewave Radio telescope (GMRT) in August 2004 at a frequency of 610 MHz. The observations have a resolution of $\sim 6.7''$ and a 5σ rms sensitivity ranging from 1.5 mJy to 2.5 mJy across the observed field. Tasse et al. (2007) detect 767 radio sources in this field and obtain estimates or upper limits for the spectral indices of these sources by comparison with the NRAO VLA Sky Survey (NVSS).

3 K-BAND DATA

We match the radio sources detected in the XMM-LSS field with K-band sources detected in the 7th data release (DR7) of the ongoing UKIRT Infrared Deep Sky Survey (UKIDSS) (Lawrence et al. 2007). UKIDSS uses the Wide Field Camera mounted on the UK Infrared Telescope (UKIRT) (Casali et al. 2007). This survey, which began in May 2005, comprises 5 complementary sub-surveys of varying depths and sky coverage. Our study uses data from the Deep extragalactic survey (DXS) which is a deep, wide
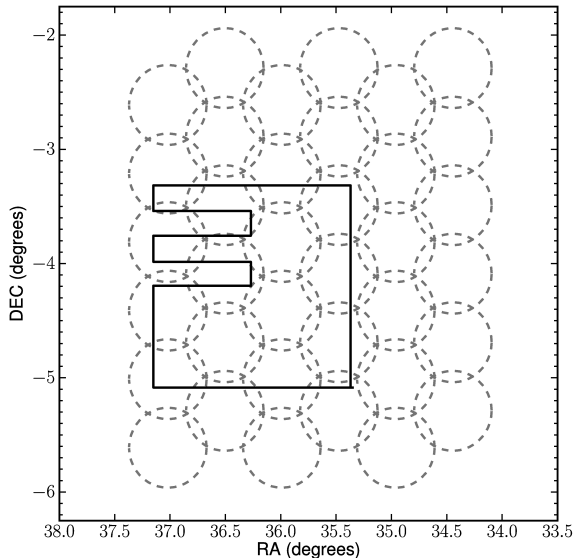
Figure 1. The location of the radio and infrared data used in this paper. The light grey circles show the 610 MHz pointings of the GMRT. The thick black line indicates the UKIDSS DXS coverage of the XMM-LSS field in the 7th data release.

survey over four observed fields. The survey is aiming to cover 35 degrees^2 to a planned 5σ depth of K∼20.8 (see e.g. Kim et al. 2010). We use the online catalogue of sources in the XMM-LSS field, the sky coverage of this field in the 7th data release is illustrated in figure 1,the overlap in the DXS sky coverage and the radio observations is approximately 2.75 degrees^2. This data is complete down to K=19.2 (Kim et al. 2010) and varies in depth across the observed field. Thus to ensure completeness we adopt a cut-off of $K > 19.2$ for the optical counterparts to our radio sources. K-band magnitudes in the UKIDSS survey are calibrated in the Vega system described by Hewett et al. (2006)

4 RADIO AND INFRARED MATCHING

For the purposes of identifying near-infrared counterparts to the radio data we divide the radio data into two categories. The first category comprises sources whose radio and optical emission are expected to be physically co-incident and includes all single component radio sources as well as partially resolved multiple component sources and double radio sources with clear radio cores. The second category contains sources where the optical emission is expected to be separated from the radio emission, this includes double radio sources with no detected radio core, radio jets and other complex multiple component structures.

To determine the optimal pairing radius for sources in the first category we consider the accuracy of the radio and K-band source positions. The radio source positions in the catalogue we use are accurate to approximately 2″ (Tasse et al. 2007) and the UKIRT survey provides accurate astrometry to within 0.1″ (Lawrence et al. 2007). We thus adopt a pairing radius of 5″, corresponding to roughly 2.5σ, where σ is the combined error in the positions of the radio and K-band sources. This large radius ensures relatively few

true optical counterparts will be located outside our search area. However as the surface density of optical sources increases there is an increasing probability that an an optical counterpart may appear within our adopted search radius by chance. To determine the probability of a given optical counterpart being such a spurious alignment we use the method of Downes et al. (1986). This method calculates the probability P that an optical source could lie at the given distance from the radio source by correcting the raw possionian probability for the number of ways that such an apparently significant association could take place. We reject all matches whose corrected probability value P> 0.05. As a further consistency check we plotted the contours of all the radio sources in DXS XMM-LSS field over the optical images and inspected the data by eye.

Determining the optical counterparts of the more complex radio sources in our second category is much less suited to statistical methods. Thus we determined the best match for sources in this category by means of visual inspection. We find matches brighter than K=19.2 for 131 sources out of a total of 213 radio sources detected in the DXS XMM-LSS field.

5 ESTIMATING REDSHIFTS

We use a method of redshift estimation, developed by Cruz et al. (2007), which utilises the tight correlation between K-band magnitude and redshift for radio galaxies. This K-z relation has been investigated for a number of radio galaxy samples including the 3CRR (Lilly & Longair 1984), 6CE (Eales et al. 1997), 6C* (Jarvis et al. 2001a) and 7CRS samples (Willott et al. 2003) and continues to at least z=3 (Jarvis et al. 2001a).

The method developed in Cruz et al. (2007) uses a model of the distribution of radio galaxies as a function of redshift together with the linear $K - z$ relation to generate a Monte Carlo simulation of radio sources which populate a synthetic $K - z$ diagram. The advantage of this method over simply applying a linear fit to the $K - z$ relation is that it incorporates information about the scatter in this relation and is thus able to provide a measure of the uncertainty in the output redshift estimates.

The distribution of radio galaxies and $K - z$ relation used in our simulations were based on the combined dataset of the 3CRR,6CE,6C* and 7CRS samples. Cruz et al. (2007) find the radio galaxies in this sample to be well fitted by a function of the form :

$$n(z) = A \exp\{-[\Sigma_{i=0}^{5} a_i (\log_{10} z)^i]^2\} \qquad (1)$$

with polynomial coefficients :

A=197.96; a_0=-0.39; a_2=1.00; a_4=1.47;
            a_1=1.17; a_3=1.83; a_5=0.38.

Willott et al. (2003) quote the best fit to the $K - z$ relation in this combined sample as the second-order polynomial

$$K(z) = 17.37 + 4.53 \log_{10} z + 0.31 (\log_{10} z)^2. \qquad (2)$$

The Monte Carlo simulations assume Gaussian deviations about a mean K-magnitude obtained from the $K-z$ relation. A constant dispersion for these deviations is adopted

for the entire redshift range. We use the dispersion σ_k obtained by Cruz et al. (2007) via a fit to the same dataset used to obtain the $K - z$ relation. This dispersion was found to be $\sigma_k = 0.593$.

The highly populated synthetic $K - z$ diagram generated by the Monte Carlo simulations can be used to obtain a photometric redshift probability density function for a source of any given K-band magnitude. This is achieved by extracting the redshifts of all the simulated sources in a narrow interval about the K-band magnitude in question. A fit to the distribution of these extracted redshifts provides the required probability density function. These distributions are best-fit by a $\log_{10}$-normal distribution with probability density function given by :

$$p(z|K) = \frac{1}{\ln(10)z\sqrt{2\pi\sigma^2}} \exp\left\{-\frac{[\log_{10}(z) - \mu]^2}{2\sigma^2}\right\} \quad (3)$$

where μ and σ are the mean and standard deviation for normally distributed random variable $\log_{10}(z)$. The best-fitting estimate for z is defined as

$$z_{est} = 10^\mu \quad (4)$$

and the asymmetric 68% confidence interval is defined as :

$$10^{\mu-\sigma} \leq z_{est} \leq 10^{\mu+\sigma} \quad (5)$$

The distribution of the estimated redshifts for all the radio sources in our survey with $K-$band counterparts is shown in figure 2. This distribution is compared with the redshift distribution predicted by the SKADS simulations (Wilman et al. 2008; Wilman et al. 2010) for a radio continuum survey with flux limits comparable to the survey used in this analysis.

This method of redshift estimation does not adjust for the possibility that optical host galaxy luminosity and radio luminosity may be correlated (e.g. Willott et al. 2003). This would most likely occur as a result of a correlation between both these properties with the mass of the central black hole. McLure et al. (2004) investigated the relationship between radio luminosity and black hole mass and concluded that these properties were only significantly correlated for the higher luminosity FRII and HERG sources, and the effect is relatively small. As we are predominantly interested in investigating the evolution of low luminosity sources in this analysis we are confident that this will not have a significant effect on our conclusions.

Although using this method essentially precludes us from investigating any correlations between galaxy mass and radio emission, (e.g. Willott et al. 2003; McLure et al. 2004), it does allow us the possiblility of just using single band photometry to measure the evolution of radio sources, and is therefore much less telescope intensive than using multiband photometry. This is particularly true if one wants to constrain the brighter end of the luminosity function, and therefore driven to use larger survey areas.

6 $\mathbf{V/V}_{\mathrm{MAX}}$

The evolution of the comoving space density of sources in a complete sample can be assessed using the non-parametric $V/V_{\max}$ method (Rowan-Robinson 1968; Schmidt 1968). Here V is the volume enclosed by the object and $V_{\max}$ is
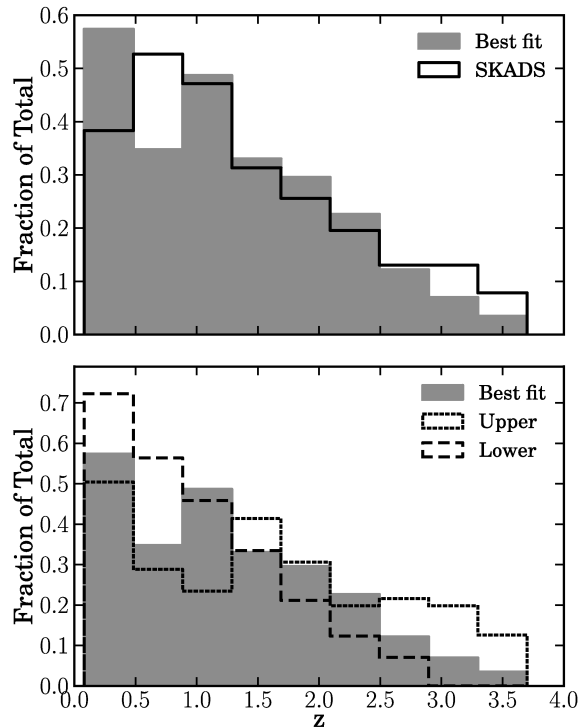

Figure 2. The distribution of the estimated redshifts of the matched radio sources in our sample. The top figure compares the best fit redshift estimates determined by our method to the theoretical redshift distribution in the SKADS simulations (Wilman et al. 2008) of a radio survey the same flux limits as that described in section 2. The bottom figure compares the best fit distribution to the distributions which would occur if all the sources had redshifts corresponding to the upper and lower 68% confidence intervals of their predicted redshift.

the volume enclosed by the object if it were located at the redshift $z_{\max}$ where it's measured flux drops below the limit of the survey. In order to determine $z_{\max}$ it is necessary to take into account flux density limits of the radio survey and the limiting magnitude of the infrared survey. If $z_{\max}$ determined by the radio data is larger than the redshift z_{opt} which would cause the source to drop out of the infrared survey then $z_{\max} = z_{opt}$. We use our Monte Carlo simulations of the K-z diagram to predict z_{opt}. We obtain a value of $z_{opt} = 2.5$ as the mean z corresponding to our limiting K-band magnitude of 19.2.

If the objects in our sample are uniformly disributed in space then $V/V_{\max}$ will be uniformly distributed between 0 and 1 with a mean value of $\langle V/V_{\max}\rangle = 0.5\pm(12N)^{-\frac{1}{2}}$, where N is the number of objects in the sample. A value of $\langle V/V_{\max}\rangle > 0.5$ implies that comoving space density of sources increases at higher redshifts ie negative evolution with cosmic time whereas $\langle V/V_{\max}\rangle > 0.5$ indicates a decline in space density with increasing redshift.

The original $\langle V/V_{\max}\rangle$ test was formulated for a single sample complete above a given radio flux density and optical magnitude. However the radio survey used in this analysis is inhomogeneous in depth (Tasse et al. 2007), thus it is more appropriate to use the generalised V_e/V_a test devised by Avni & Bahcall (1980) to analyse the evolutionary
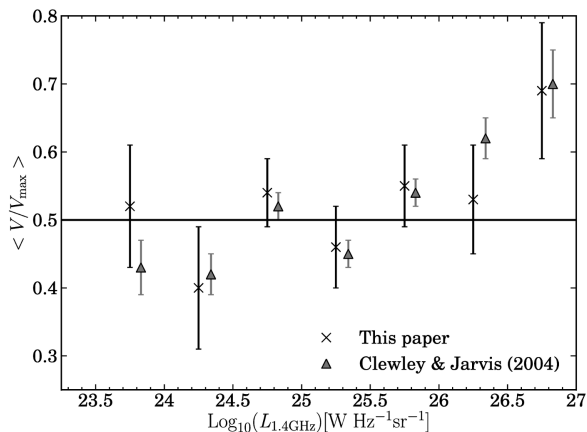
Figure 3. Average V/V_{max} in seven different radio luminosity bins compared to the results obtained in Clewley & Jarvis (2004).

$L_{1.4\mathrm{GHz}}$ [W Hz^{-1}sr^{-1}]	$\langle V_e/V_a \rangle$	1σ	1σ (MC)	$\langle z \rangle$
23.5-24	0.52	0.09	0.07	0.26
24-24.5	0.40	0.09	0.06	0.47
24.5-25	0.55	0.05	0.04	0.91
25-25.5	0.46	0.06	0.04	1.2
25.5-26	0.55	0.06	0.05	1.7
26-26.5	0.53	0.08	0.06	1.7
26.5-27	0.69	0.10	0.07	1.9

Table 1. Results of $\langle V_e/V_a \rangle$ analysis is seven luminosity bins. The column entitled 1σ (MC) quotes the uncertainty in our $\langle V/V_{max} \rangle$ estimates due to the uncertainty in our redshift estimates. The last column gives the mean z of sources in each bin.
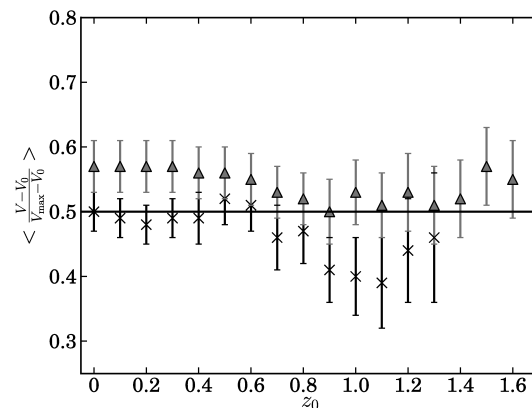

Figure 4. The banded V/V_{max} in two luminosity bins. The bin with $L_{1.4\mathrm{GHz}} > 10^{25}$ W Hz^{-1}sr^{-1} is represented by grey triangles and the black crosses represent the $L_{1.4\mathrm{GHz}} < 10^{25}$ W Hz^{-1}sr^{-1} bin.

properties of this sample. The generalised test treats the incomplete radio data as a single sample with a variable survey area. This variable survey area depends on the flux density of the individual radio source. The new test variables are the enclosed volume V_e and the available volume V_a, the statistical properties of the V_e/V_a variable are identical to those of the V/V_{max} variable in a single flux-limited sample (Avni & Bahcall 1980).

To determine the effective survey area as a function of radio flux density we perform a simple simulation. We inject a 1000 radio sources with peak flux densities ranging from 1-4 mJy into the original map of the radio data. These simulated sources are restricted to the 2.75 degrees^2 covered by the DXS survey. We determine the fraction of these simulated sources which are recovered by the source extraction algorithm SAD in the Astronomical Image Processing Software (AIPS) as a function of their input flux densities.

7 V/V_{MAX} RESULTS

In figure 3 we compare the mean V_e/V_a statitistics obtained in our analysis with those found in Clewley & Jarvis (2004). We find that our results are in agreement with their analysis which is based on galaxies selected at 325 Mhz in the Sloan Digital Sky Survey. Our results also compare very well with the V/V_{max} results of Tasse et al. (2008). Their analysis is based on a combination of 325 MHz and 610 MHz radio sources in the XMM-LSS field, the data used in their analysis overlaps the DXS field studied in this paper so it is encouraging that we obtain a similar result. The strong evolution of the high luminosity radio sources detected by Clewley & Jarvis (2004) is also in evidence in our figure 3 although this result is at a lower statistical significance due to the small size of our sample, similarly their is a little evidence that the low power sources are evolving with cosmic time. The 610 MHz flux densities of our radio sources were converted to 1.4 GHz radio luminosities using the spectral index estimates obtained by Tasse et al. (2007) by comparision with the NVSS survey.

As discussed in section 5, there is some uncertainty in the redshift estimates used in this analysis due to the in-

herent scatter in the $K - z$ relation. To characterise the effect of this source of error on our V_e/V_a estimates we use Monte Carlo methods. In these Monte Carlo simulations we assign each source a redshift estimate determined by the redshift probability density function derived from its' K-band magnitude. We use these simulated redshifts to rederive the $\langle V_e/V_a \rangle$ in the seven luminosity bins in figure 3. We repeat this process 1000 times to obtain the 68% confidence interval of the V_e/V_a estimates. This confidence interval is indicated in table 1 . The size of this source of error is comparable to the statistical errors due to the sample size.

To further our investigation of this evolutionary behaviour we determine the banded V_e/V_a statistic in two luminosity bins. A high luminosity bin corresponding to sources with $L_{1.4\mathrm{GHz}} > 10^{25}$ W Hz^{-1}sr^{-1} and a low luminosity bin with $L_{1.4\mathrm{GHz}} < 10^{25}$ W Hz^{-1}sr^{-1}. The banded test calculates the mean V_e/V_a for all sources with $z > z_0$ for a range of z_0 values. All evolution below z_0 is thus masked out of the analysis allowing us to determine whether the evolution of these two populations of radio sources changes as a function of redshift. The results of the banded test are presented in figure 4. The error in the banded test as a result of the uncertainty in our redshift estimates is also calculated using Monte Carlo methods and presented in table 7.

The results in figure 4 indicate that there is little evidence of evolution in the low power radio sources out to

	$L_{1.4\mathrm{GHz}} < 10^{25}$ W Hz^{-1}sr^{-1}			$L_{1.4\mathrm{GHz}} > 10^{25}$ W Hz^{-1}sr^{-1}		
z_0	$\langle V_e/V_a \rangle$	1σ	1σ(MC)	$\langle V_e/V_a \rangle$	1σ	1σ (MC)
0	0.50	0.03	0.02	0.57	0.04	0.02
0.2	0.48	0.03	0.02	0.57	0.04	0.02
0.4	0.49	0.04	0.04	0.56	0.04	0.03
0.6	0.51	0.04	0.05	0.55	0.04	0.03
0.8	0.47	0.05	0.07	0.52	0.04	0.03
1.0	0.40	0.05	0.14	0.53	0.05	0.04
1.2	0.44	0.08	0.24	0.53	0.05	0.05
1.4				0.52	0.06	0.05
1.6				0.55	0.05	0.06

Table 2. Results of the banded $\langle V_e/V_a \rangle$ test. The columns entitled 1σ (MC) list the Monte Carlo estimates of the error in our $\langle V_e/V_a \rangle$ estimates due to scatter in the $K-z$ relation.

a redshift of $z \sim 0.8$. Beyond this redshift there is a slight decline in the average V_e/V_a of this population however the errors derived from our Monte Carlo estimates increase significantly at these higher redshifts. The stronger evolution of the high luminosity sources can also be seen in this figure. The mean V_e/V_a for the low and high luminosity bins is calculated as 0.5 ± 0.03 and 0.57 ± 0.04 respectively.

8   RADIO LUMINOSITY FUNCTION

Another standard means of quantifying the cosmic evolution of radio sources is to compare the measured radio luminosity function (LF) of these sources at different cosmic epochs. Changes in the luminosity function $\Phi_z(L)$ are usually modelled as being due to one of two simplified evolution scenarios, either pure density evolution or pure luminosity evolution. In pure density evolution the luminosity distribution of the radio sources is considered fixed while the number density of radio sources changes with redshift. In this scenario the measured LF at a given redshift $\Phi_z(L)$ is related to the local luminosity function $\Phi_0(L)$ via the following equation :

$$\Phi_z(L) = (1 + z)^{\alpha_D} \Phi_0(L) \qquad (6)$$

In pure luminosity evolution the radio sources undergo a change in their luminosity with time, this evolution is parameterized as:

$$\Phi_z(L) = \Phi_0 \left(\frac{L}{(1+z)^{\alpha_L}} \right) \qquad (7)$$

We calculate the $\Phi_z(L)$ of our sample in four redshift bins using the standard $1/V_{max}$ method of Schmidt (1968). Thus the radio LF and its corresponding error is calculated for a particular luminosity bin as:

$$\Phi(L) = \sum_{j=1}^{N} \frac{1}{V_{\max}^j} \qquad \sigma = \sqrt{\sum_{j=1}^{N} \left(\frac{1}{V_{\max}^j} \right)^2} \qquad (8)$$

where the j index runs over all sources in the luminosity bin L-ΔL $\rightarrow$L+ΔL. We adjust the V_{max} values to take into account the redshift limits of the four redshift bins for which the luminosity functions were calculated. The results of our analysis are presented in figure 5 and compared with the LF of radio sources in the VLA-COSMOS survey derived
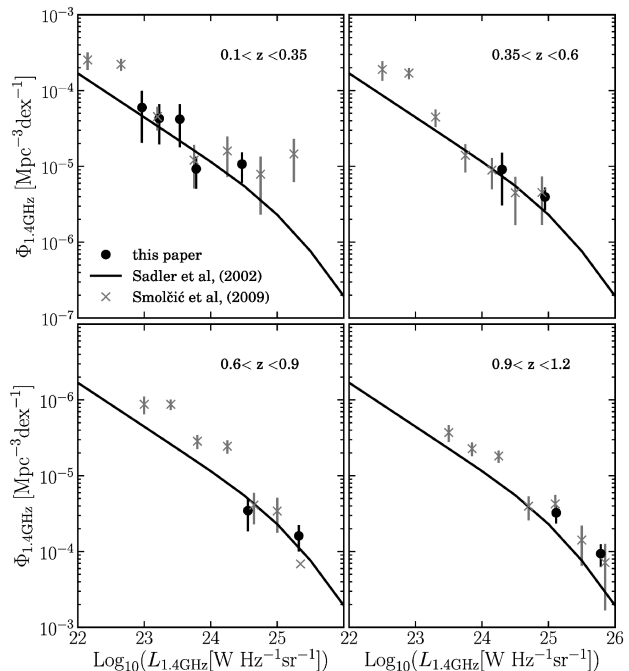

Figure 5. The measured radio luminosity function in four redshift bins compared to the results of Smolčić et al. (2009). The solid line represents the analytic form of the local luminosity function derived in Sadler et al. (2002).

by Smolčić et al. (2009). Our luminosity function estimates appear to be in good agreement with the results of this previous study.

Smolčić et al. (2009) characterise the evolution of the radio sources in the VLA-COSMOS survey by adopting the LF given by Sadler et al. (2002) as the best representative of their measured local luminosity function and using a least squares fit to derive the α_D and α_L parameters for pure density and pure luminosity evolution of this LF. The analytic form of the radio LF given in Sadler et al. (2002) was obtained from radio galaxies in the NVSS survey matched with optical counterparts in the 2dF Galaxy Redshift Survey.

The fitting procedure of Smolčić et al. (2009) yeilded estimates of $\alpha_D = 1.1 \pm 0.1$ and $\alpha_L = 0.8 \pm 0.1$ where the errors were derived from the distribution of χ^2 in the least squares fit. Employing this same method we obtain values for the density and luminosity evolution parameters of $\alpha_D = 0.6 \pm 0.1$ and $\alpha_L = 0.8 \pm 0.2$. These estimates are fairly consistent with the estimates of Smolčić et al. (2009) and imply an increase in the co-moving space density of low luminosity radio sources by a factor of ~ 1.5 in the interval between z=0 $-$ 0.8.

The consistency of our results with those of Smolčić et al. (2009) provides encouranging evidence that the $K-z$ relation can be used to investigate the radio luminosity function. This could provide a useful alternative technique for studying the LF in the absence of multi-band photometric redshift estimates.

9 CONCLUSION

We have used the non-parametric V/V_{max} test and the radio luminosity function to investigate the the cosmic evolution of low power radio sources in the XMM-LSS field. Previous investigations of the evolution of low-power radio sources have found evidence of mild evolution taking place in the redshift range $z = 0 - 1.3$. Donoso et al. (2009) find that the co-moving density of low luminosity sources ($L_{1.4GHz} < 10^{25}$ W Hz^{-1}sr^{-1}) in the MegaZ-Luminous Red Galaxy catalogue increases by a factor of 1.5 between $z = 0.1 - 0.55$. Similarly Sadler et al. (2007) find evidence that low luminosity sources experience mild evolution with an increase in their number density by a factor of $\sim$2 at z=0.55. This is significantly less than the strong evolution detected in the high power radio sources whose number densities are enhanced by a factor of 10 in the same cosmic timeframe. The results of Sadler et al. (2007) seem to rule out the no-evolultion scenario. Gendre et al. (2010) find evidence that higher luminosity, $L_{1.4GHz} \geq 10^{24.5}$ W Hz^{-1}sr^{-1} FRI

Smolčić et al. (2009) find mild evolution of the low power AGN in the VLA-COSMOS survey out to $z \sim 1.3$. Our results are broadly consistent with these previous works and imply density enhancements by a factor $\sim$ 1.5 at z=0.8. This is slightly less than the evolution implied in Sadler et al. (2007), but in fairly good agreement with the estimates in Smolčić et al. (2009) and Donoso et al. (2009). We also find evidence that the low power radio AGN are evolving more slowly than their high power counterparts in the redshift range $z = 0 - 0.8$ and tentative evidence that this separation in evolutionary behaviour persists to $z = 1.2$.

The division in the FRI/FRII classification system and the LERG/HERG system occurs at roughly the same luminosity threshold of $L_{1.4GHz} \sim 10^{25}$. As our analysis categorises our radio sources solely on their luminosity we are unable to determine whether the separation in evolutionary behaviour is due to the FRI/FRII dichotomy or to differences in black hole accretion modes in HERGS and LERGS.

Our results demonstrate that using the $K-$band (or similar wavelength), combined with radio surveys, is a viable route to investigating the evolution of the radio source population, at least up to $z \sim 1.2$. In the future, all-sky radio surveys such as those carried out with the Low-Frequency Array (LOFAR; Morganti et al. 2010) and the Australian Square Kilometre Array Pathfinder (ASKAP) telescope, combined with the UKIDSS large area survey and the VISTA Hemisphere Survey, as well as Wide-field Infrared Survey Explorer (WISE), will enable us to pin down the evolution of the radio source population to a much higher degree of accuracy.

REFERENCES

Avni Y., Bahcall J. N., 1980, ApJ, 235, 694

Best P. N., Kaiser C. R., Heckman T. M., Kauffmann G., 2006, MNRAS, 368, L67

Bîrzan L., Rafferty D. A., McNamara B. R., Wise M. W., Nulsen P. E. J., 2004, ApJ, 607, 800

Bower R. G., Benson A. J., Malbon R., Helly J. C., Frenk C. S., Baugh C. M., Cole S., Lacey C. G., 2006, MNRAS, 370, 645

Casali M. et al, 2007, A & A, 467, 777

Clewley L., Jarvis M. J., 2004, MNRAS, 352, 909

Croton D. J., Springel V., White S. D. M., De Lucia G., Frenk C. S., Gao L., Jenkins A., Kauffmann G., Navarro J. F., Yoshida N., 2006, MNRAS, 365, 11

Cruz M. J., Jarvis M. J., Rawlings S., Blundell K. M., 2007, MNRAS, 375, 1349

Donoso E., Best P. N., Kauffmann G., 2009, MNRAS, 392, 617

Doroshkevich A. G., Longair M. S., Zeldovich Y. B., 1970, MNRAS, 147, 139

Downes A. J. B., Peacock J. A., Savage A., Carrie D. R., 1986, MNRAS, 218, 31

Dunlop J. S., Peacock J. A., 1990, MNRAS, 247, 19

Eales S., Rawlings S., Law-Green D., Cotter G., Lacy M., 1997, MNRAS, 291, 593

Evans D. A., Worrall D. M., Hardcastle M. J., Kraft R. P., Birkinshaw M., 2006, ApJ, 642, 96

Fabian A. C., Sanders J. S., Crawford C. S., Conselice C. J., Gallagher J. S., Wyse R. F. G., 2003, MNRAS, 344, L48

Fanaroff B. L., Riley J. M., 1974, MNRAS, 167, 31P

Gendre M. A., Best P. N., Wall J. V., 2010, MNRAS, 4040, 1719

Gendre M. A., Wall J. V., 2008, MNRAS, 390, 819

Hardcastle M. J., Evans D. A., Croston J. H., 2006, MNRAS, 370, 1893

Hardcastle M. J., Evans D. A., Croston J. H., 2007, MNRAS, 376, 1849

Herbert, P. D., Jarvis, M. J., Willott, C. J., McLure, R. J., Mitchell, E., Rawlings, S., Hill, G. J., & Dunlop, J. S. 2010, MNRAS, 406, 1841

Hewett P. C.,Warren S. J.,Leggett S. K.,Hodgkin S. T., 2006, MNRAS, 367, 454

Hine, R. G., & Longair, M. S. 1979, MNRAS, 188, 111

Jackson, N., & Rawlings, S. 1997, MNRAS, 286, 241

Jackson C. A., Wall J. V., 1999, MNRAS, 304, 160

Jarvis, M. J., & McLure, R. J. 2002, MNRAS, 336, L38

Jarvis, M. J., & Rawlings, S. 2000, MNRAS, 319, 121

Jarvis M. J., Rawlings S., Eales S., Blundell K. M., Bunker A. J., Croft S., McLure R. J., Willott C. J., 2001a, MNRAS, 326, 1585

Jarvis, M. J., Rawlings, S., Willott, C. J., Blundell, K. M., Eales, S., & Lacy, M. 2001b, MNRAS, 327, 907

Kim, J.-W., Edge, A. C., Wake, D. A., & Stott, J. P. 2010, MNRAS, 1421

Laing R. A., Jenkins C. R., Wall J. V., Unger S. W., 1994, in G. V. Bicknell, M. A. Dopita, & P. J. Quinn eds., Proc. PASP. 54, The Physics of Active Galaxies. p 201

Laing R. A., Riley J. M., Longair M. S., 1983, MNRAS, 204, 151

Lawrence A. et al, 2007, MNRAS, 379, 1599

Ledlow M. J., Owen F. N., 1996, AJ, 112, 9

Lilly S. J., Longair M. S., 1984, MNRAS, 211, 833

Longair M. S., 1966, MNRAS, 133, 421

McLure, R. J., Willott, C. J., Jarvis, M. J., Rawlings, S., Hill, G. J., Mitchell, E., Dunlop, J. S., & Wold, M. 2004, MNRAS, 351, 347

Morganti, R., et al. 2010, arXiv:1001.2384

Rawlings S., Jarvis M. J., 2004, MNRAS, 355, L9

Rigby E. E., Snellen I. A. G., Best P. N., 2007, MNRAS, 380, 1449

Rowan-Robinson M., 1968, MNRAS, 138, 445

Sadler E. M. et al, 2007, MNRAS, 381, 211

Sadler E. M. et al, 2002, MNRAS, 329, 227

Schmidt M., 1968, ApJ, 151, 393

Smolčić V. et al, 2009, ApJ, 696, 24

Tasse C., Best P. N., Röttgering H., Le Borgne D., 2008, A & A, 490, 893

Wall, J. V., Jackson, C. A., Shaver, P. A., Hook, I. M., & Kellermann, K. I. 2005, A&A, 434, 133

Tasse C., Röttgering H. J. A., Best P. N., Cohen A. S., Pierre M., Wilman R., 2007, A & A, 471, 1105

Waddington I., Dunlop J. S., Peacock J. A., Windhorst R. A., 2001, MNRAS, 328, 882

Willott C. J., Rawlings S., Blundell K. M., Lacy M., Eales S. A., 2001, MNRAS, 322, 536

Willott C. J., Rawlings S., Jarvis M. J., Blundell K. M., 2003, MNRAS, 339, 173

Wilman R. J., et al., 2008, MNRAS, 338, 1335

Wilman, R. J., Jarvis, M. J., Mauch, T., Rawlings, S., & Hickey, S. 2010, MNRAS, 405, 447